WAMS-BASED MODE METERS WITH GUARANTEES ON DATA RECOVERY UNDER CORRUPTION

Dr. Nilanjan Ray Chaudhuri

Associate Professor

School of Electrical Engineering and Computer Science

Pennsylvania State University, University Park, PA

SUstainable Power & Energy Research Group (SUPER Group)

Thrust I: PMU Data Anomaly Detection & Correction

Thrust II: Wide-Area Damping Control

Thrust III: HVDC and MTDC

Thrust IV: Coupled Cascading Failure

PennState
College of Engineering

SUPER Group Team

Kaustav Chatterjee
Ph.D. Student

Sina Gharebaghi
Ph.D. Student

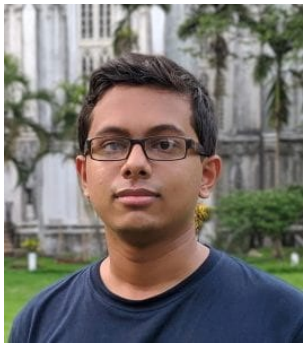

Sayan Samanta
Ph.D. Student

Outline

- Corruption resilience in absence of complete system observability
- RPCA basics for anomaly detection and correction in PMU data
- Guarantees for exact signal recovery
- Corruption-resilient signal selection: propositions and lemmas
- Case studies: simulated and field PMU data

Dr. Kaveri Mahapatra
Alumnus: SUPERgroup

Kaustav Chatterjee
Ph.D. Student

Abundance of PMUs in North America

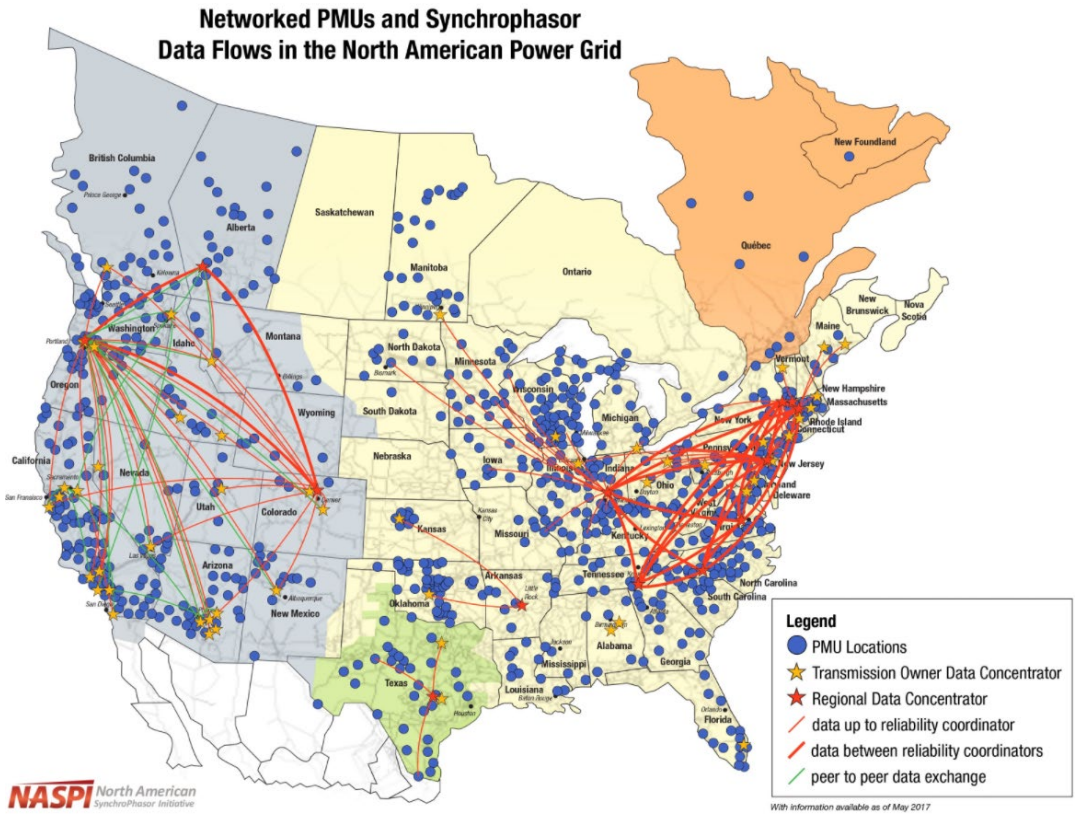

- In 2017: over 2,500 networked PMUs in North America
- Most Reliability Coordinators receiving and sharing PMU data for wide-area monitoring
- More time needed before complete observability is achieved

We have some distance to cover before full observability through PMUs is achieved

Application of Wide Area Monitoring

- Example applications requiring full observability:
  - 'Dynamic' state estimation
  - Voltage stability assessment in a meshed network
- Example applications not requiring full observability:
  - 'Dynamic state' estimation
  - Oscillation monitoring through 'mode meters'
- Mode meters already operational in control centers
  - California ISO, PG&E, BPA, and TVA
  - Web-based version deployed in 7 operations centers and 11 reliability coordinators

Mode meters estimate damping ratios and frequencies of oscillations

Literature Review

- Data anomaly detection/correction:
  - State estimation-based: needs full observability (examples)

[A] Y. Gu et-al , "Bad Data Detection Method for Smart Grids based on Distributed State Estimation," in 2013 IEEE International Conference on Communications (ICC), Jun. 2013, pp. 4483–4487.
[B] A. S. Dobakhshari and A. M. Ranjbar, "A Wide-Area Scheme for Power System Fault Location Incorporating Bad Data Detection," IEEE Trans. Power Del., vol. 30, no. 2, pp. 800–808, 2015.
[C] S. Cui, Z. Han, S. Kar, T. T. Kim, H. V. Poor, and A. Tajer, "Coordinated data-injection attack and detection in the smart grid: A detailed look at enriching detection solutions," IEEE Signal Processing Magazine, vol. 29, no. 5, pp. 106–115, Sep. 2012.
[D] T. A, S. Sihag et-al "Non-linear state recovery in power system under bad data and cyber attacks," Journal of Modern Power Systems and Clean Energy, vol. 7, no. 5, pp. 1071–1080, 2019.
[E] A. Ashok et-al "Online Detection of Stealthy False Data Injection Attacks in Power System State Estimation," IEEE Trans. Smart Grid, vol. 9, no. 3, pp. 1636–1646, May 2018.

  - Measurement-driven data preprocessing: neither require full observability with PMUs, nor need network topology information (examples)

[A] Y. Hao et-al, "Modelless Data Quality Improvement of Streaming Synchrophasor Measurements by Exploiting the Low-Rank Hankel Structure," IEEE Trans. Power Syst., vol. 33, no. 6, pp. 6966–6977, Nov. 2018.
[B] P. Gao, R. Wang, M. Wang, and J. H. Chow, "Low-Rank Matrix Recovery From Noisy, Quantized, and Erroneous Measurements," IEEE Trans. Signal Process., vol. 66, pp. 2918–2932, 2018.
[C] P. Gao et-al "Missing Data Recovery for High-Dimensional Signals With Nonlinear Low-Dimensional Structures," IEEE Trans. Signal Process., vol. 65, no. 20, pp. 5421–5436, Oct. 2017.
[D] M. Liao et-al "An Alternating Direction Method of Multipliers Based Approach for PMU Data Recovery," IEEE Trans. Smart Grid, vol. 10, no. 4, pp. 4554–4565, 2019.
[E] K. Mahapatra et-al "Malicious Corruption-Resilient Wide-Area Oscillation Monitoring Using Principal Component Pursuit," IEEE Trans. Smart Grid, vol. 10, no. 2, pp. 1813–1825, 2019.
[F] ——, "Malicious Corruption-Resilient Wide-Area Oscillation Monitoring using Online Robust PCA," in 2018 IEEE Power Energy Society General Meeting (PESGM), Aug. 2018, pp. 1–5.
[G] ——, "Online Robust PCA for Malicious Attack-Resilience in Wide-Area Mode Metering Application," IEEE Trans. Power Syst., vol. 34, no. 4, pp. 2598–2610, Jul. 2019.
[H] K. Chatterjee et-al "Robust Recovery of PMU Signals with Outlier Characterization and Stochastic Subspace Selection," IEEE Trans. Smart Grid, pp. 1–1, 2019.

We focus on second approach: exploit the spatiotemporal correlation

Literature Review

- Signal selection for mode metering: (A) Modal observability-based, (B) Participation ratio, (C) Power spectral density

[A] D. J. Trudnowski, “Estimating Electromechanical Mode Shape From Synchrophasor Measurements,” IEEE Trans. Power Syst., vol. 23 no. 3, pp. 1188–1195, 2008.
[B] T. Huang, M. Wu, and L. Xie, “Prioritization of PMU Location and Signal Selection for Monitoring Critical Power System Oscillations,” IEEE Trans. Power Syst., vol. 33, no. 4, pp. 3919–3929, 2018.
[C] V. S. Peri´c, X. Bombois, and L. Vanfretti, “Optimal Signal Selection for Power System Ambient Mode Estimation Using a Prediction Error Criterion,” IEEE Trans. Power Syst., vol. 31, no. 4, pp. 2621–2633, Jul. 2016.

Can we intelligently
locate the PMUs and/or group signals from installed PMUs
such that the resulting combinations guarantee data recovery
from corruption while capturing every information necessary
to estimate the critical modes?

PMU data Anomaly Detection & Correction Problem

- Anomaly example:
  - So-called 'bad data' stemming from problems in communication infrastructure
  - False data injection (FDI) attacks like: (1) Parameter manipulation, (2) Fault-resembling, (3) Missing data, (4) Data repetition
- Corruption model: $\mathbf{z}(t) = \mathbf{y}(t) + \mathbf{e}(t)$; $\mathbf{z}(t)$: corrupted, $\mathbf{y}(t)$: actual, $\mathbf{e}(t)$: corruption
- Assumption:
  - Corruption is 'sparse': a fraction of channels attacked/affected at any point in time
  - Communication layer security can be breached, control center is secure
- Note: **s-sparse vector → vector with at most s nonzero entries**
- Objective: detect the anomaly and predict $\mathbf{e}(t)$ – posed as **Sparse Recovery Problem**

Low-rank property of PMU data & sparse corruption vector are important

Robust PCA (RPCA) Basics: Sparse Recovery Problem

- $\mathbf{z}(t) = \mathbf{y}(t) + \mathbf{e}(t)$, Objective: detect the anomaly and predict $\mathbf{e}(t)$
- **Robust PCA (R-PCA)** as a tool from Compressed Sensing literature
- Consider a window of PMU data samples:

$$\mathbf{Y} = \left[\hat{\mathbf{y}}(t - N\tau) \quad \dots \quad \hat{\mathbf{y}}(t - \tau) \right] \quad \mathbf{Y} \in \Re^{n \times N} \qquad \mathbf{Y} \approx \hat{\mathbf{U}}\hat{\mathbf{\Sigma}}\hat{\mathbf{V}}^H$$

Columns of $\widehat{\boldsymbol{U}}$ and $\widehat{\boldsymbol{V}}$: left and right singular vectors for r dominant modes

- Y: Low rank for a large power grid – only r dominant directions considered in $\widehat{U}$.
- **Basic idea:** Decompose $\mathbf{z}(t)$ into estimates $\hat{y}(t)$ and $\hat{e}(t)$, such that
  - $\hat{y}(t)$ is in low-rank subspace spanned by $\widehat{U}$ and
  - $\hat{e}(t)$ is sparse corruption vector

Low-rank property of PMU data & sparse corruption vector are important

Robust PCA (RPCA) Basics: Sparse Recovery Problem

- $\mathbf{z}(t)$ projected onto space orthogonal to span of $\widehat{U}$:

$$\boldsymbol{\gamma}(t) = \boldsymbol{\Phi}\mathbf{z}(t) = \boldsymbol{\Phi}(\mathbf{y}(t) + \mathbf{e}(t)) = \boldsymbol{\Phi}\mathbf{e}(t) + \boldsymbol{\nu}(t) \qquad \boldsymbol{\Phi} = \mathbf{I} - \hat{\mathbf{U}}\hat{\mathbf{U}}^H$$

- Ideally, $\mathbf{y}(t) \in \text{span}(\widehat{U})$ implying $\boldsymbol{\Phi}\mathbf{y}(t)$ nullified.

- Actually, because of (1) measurement noise, (2) limiting $\widehat{U}$ dimension to r columns → $\boldsymbol{\Phi}\mathbf{y}(t) = \boldsymbol{\nu}(t)$: negligibly small

- Estimation of $\mathbf{e}(t)$ from $\mathbf{z}(t)$: optimization problem ensuring maximum sparsity:

$$\min_{\mathbf{e}(t)} \left\|\mathbf{e}(t)\right\|_0 \quad \text{s.t.} \quad \left\|\boldsymbol{\gamma}(t) - \boldsymbol{\Phi}\mathbf{e}(t)\right\|_2 \leq \eta(t)$$

nonconvex problem

- Convex relaxation leads to so-called LASSO problem [1]:

$$\min_{\mathbf{e}(t)} \left\|\mathbf{e}(t)\right\|_1 \quad \text{s.t.} \quad \left\|\boldsymbol{\gamma}(t) - \boldsymbol{\Phi}\mathbf{e}(t)\right\|_2 \leq \eta(t)$$

- Thresholding term: $\eta(t) = ||\boldsymbol{\Phi}\hat{\mathbf{y}}(t-\tau)||_2$

An efficient ℓ_1 solver can solve this optimization problem

[1] H. Guo, C. Qiu, and N. Vaswani, "An Online Algorithm for Separating Sparse and Low-Dimensional Signal Sequences From Their Sum," IEEE Trans. Signal Process., vol. 62, no. 16, pp. 4284–4297, Aug. 2014.

Proposed Architecture

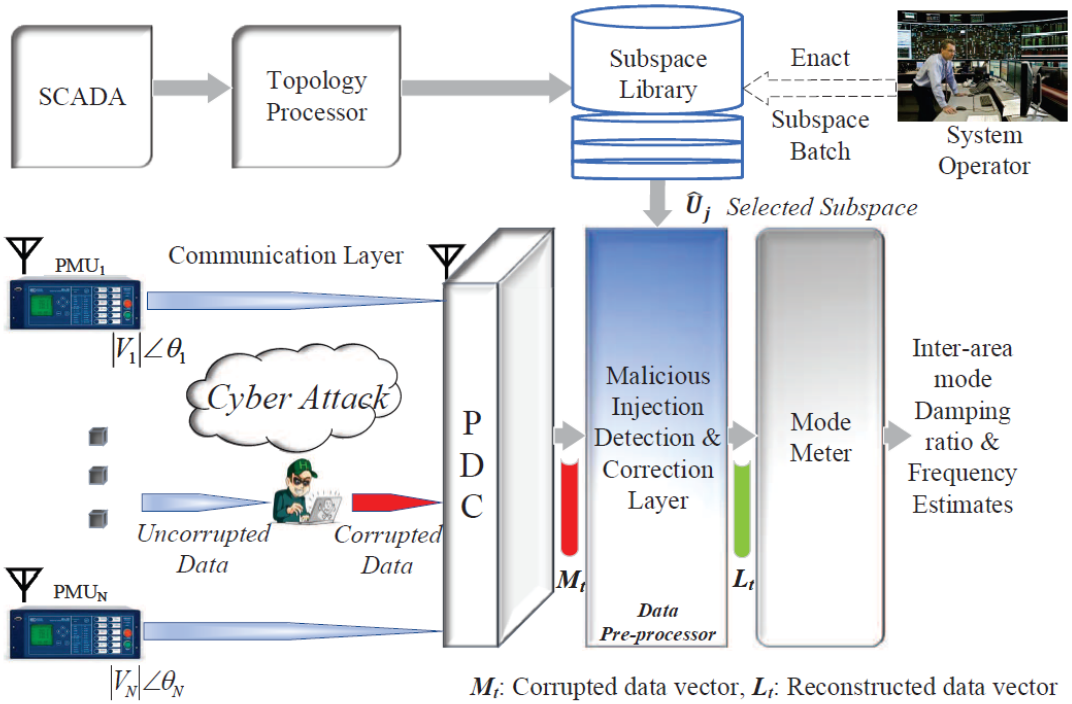

Subspace library:

- **Offline** simulation of planning models: self-clearing faults under different loading conditions
- Daily and seasonal variation to be considered: planner's experience is critical
- Perform SVD and store the dominant singular vectors from $\hat{U}$ to create each subspace
- Subspace selection: can be automated [2]

Data pre-processor takes two inputs: (1) PMU data, (2) Subspace from Library

[2] K. Chatterjee, K. Mahapatra, and N. R. Chaudhuri, "Robust Recovery of PMU Signals with Outlier Characterization and Stochastic Subspace Selection," IEEE Transactions on Smart Grid, IEEE Transactions on Smart Grid, vol. 11, no. 4, pp. 3346 – 3358.

IEEE 68 Bus New England- New York Test System

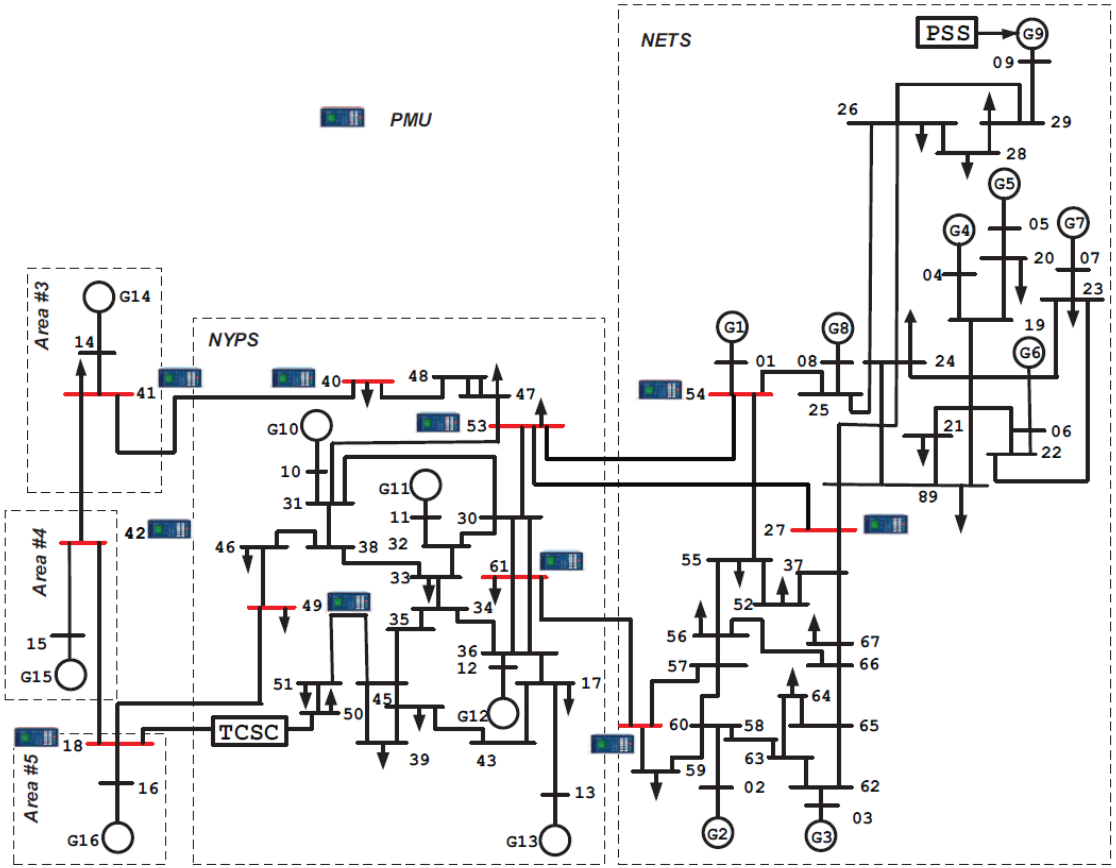

Ambient: Parameter Manipulation Attack

Injection of signals with altered modal characteristics in 20% of signals

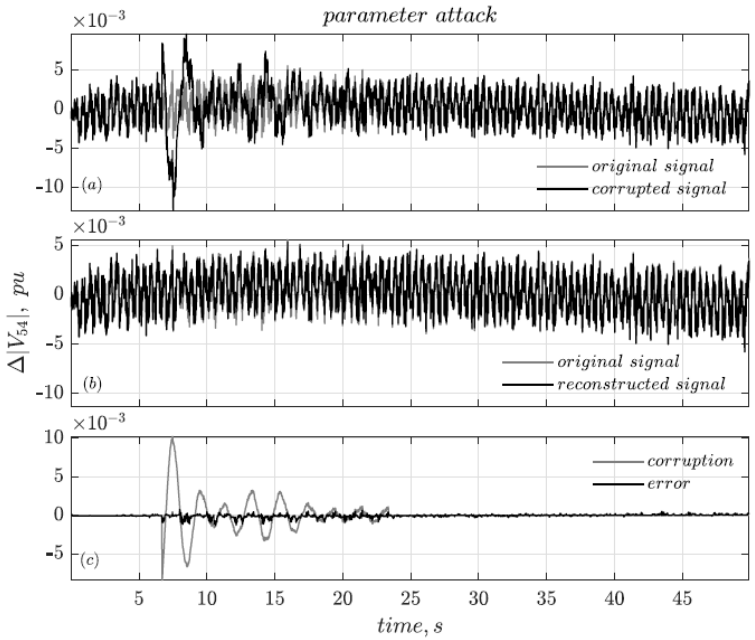

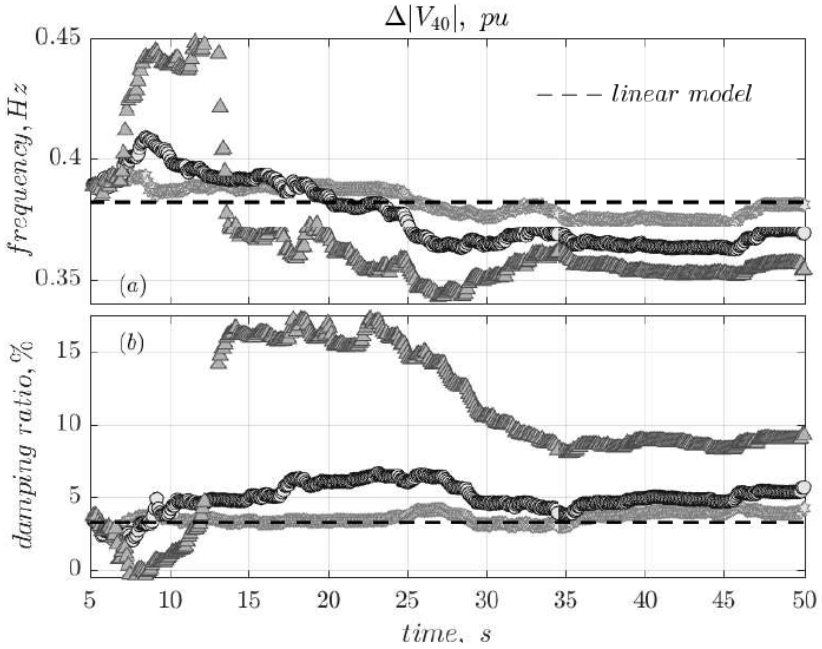

'Δ' : Corrupted, '*': Ground truth,
'o': Corrected

Ambient: Fault Resembling Injection Attack

'Playback' of fault data in 20% of signals

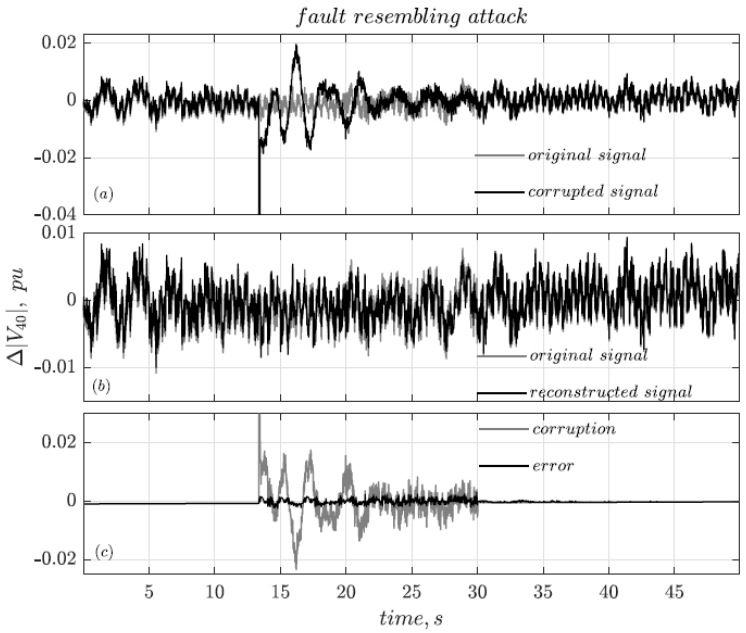

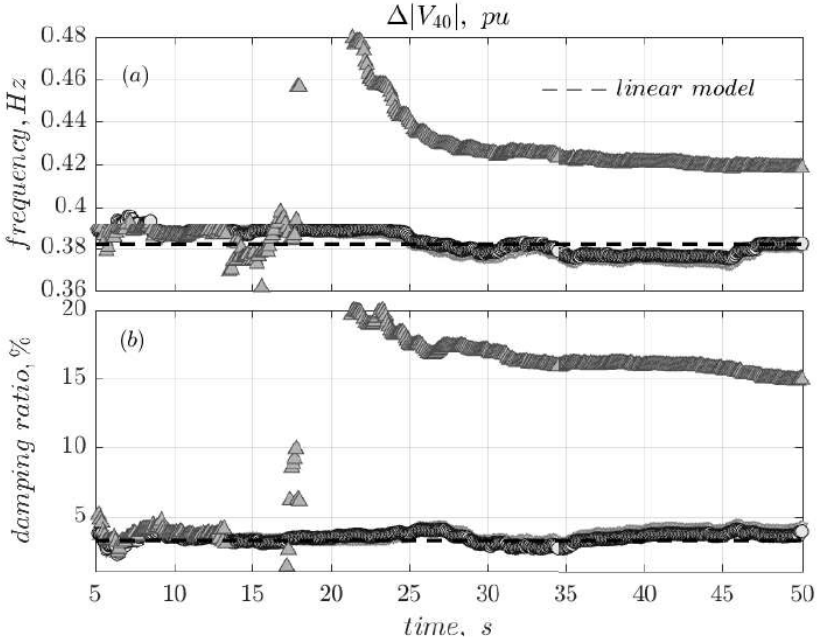

'Δ' : Corrupted, '*': Ground truth,
'o': Corrected

Transient: Missing Data & Data Repetition Attacks

Self-explanatory

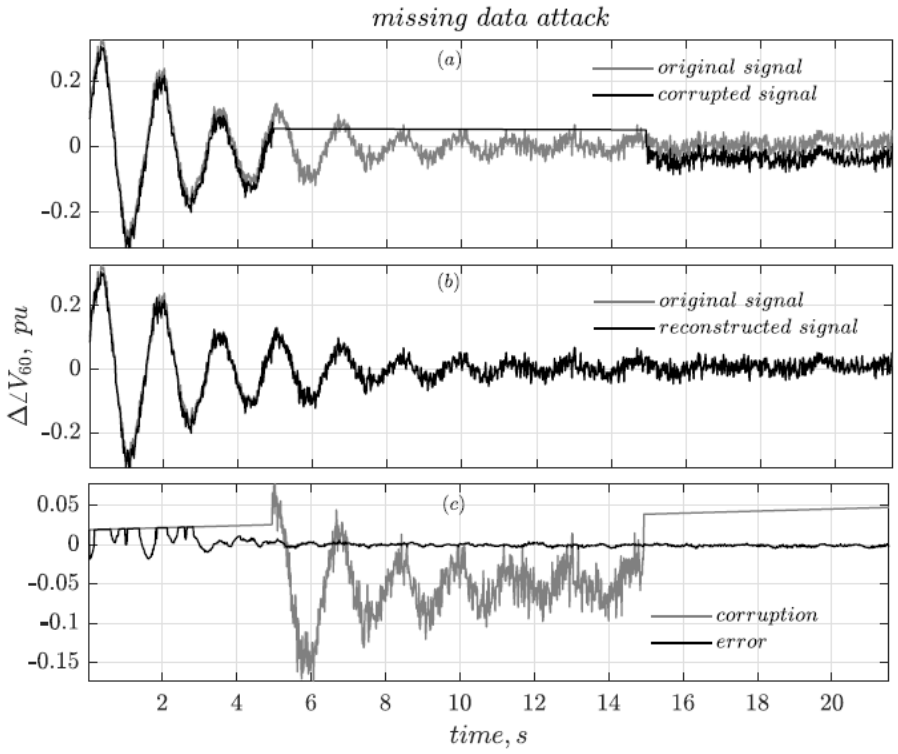

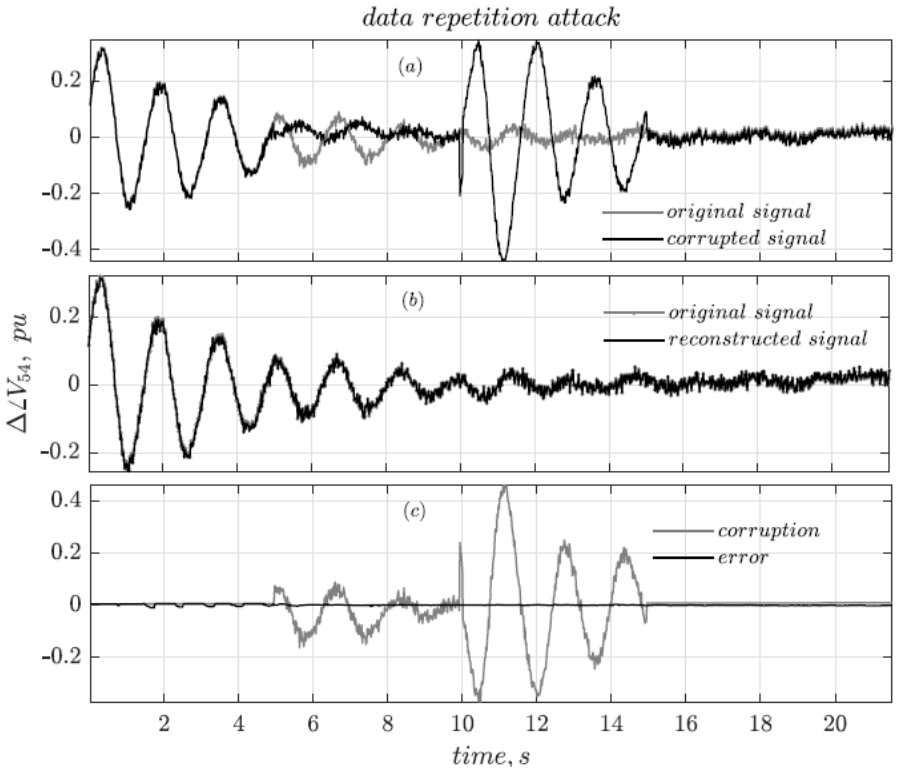

Guarantees for Exact Recovery

- Convex relaxation leads to so-called LASSO problem [3]:

$$\min_{\mathbf{e}(t)} \left\|\mathbf{e}(t)\right\|_1 \quad \text{s.t.} \quad \left\|\boldsymbol{\gamma}(t) - \boldsymbol{\Phi}\mathbf{e}(t)\right\|_2 \leq \eta(t)$$

- Exact recovery guaranteed ($\ell_0 - \ell_1$ equivalence) and a *s*-sparse solution is returned if *s*-restricted isometry constant $\delta_s(\Phi) < 0.307$ [4]: Sufficiency condition

$$\delta_s(\boldsymbol{\Phi}) = \delta_s(\mathbf{I} - \hat{\mathbf{U}}\hat{\mathbf{U}}^H) = \kappa_s(\hat{\mathbf{U}})^2$$
$$\delta_s(\boldsymbol{\Phi}) < 0.307 \implies \kappa_s(\mathbf{Y}) = \kappa_s(\hat{\mathbf{U}}) < 0.554 = \kappa^*$$

$\boldsymbol{\kappa_s(Y)}$ is the denseness coefficient: $\kappa_s(\mathbf{Y}) = \kappa_s(\text{range}(\mathbf{Y})) = \max_{|T|\leq s} \left\|(\mathbf{I}_T)^H \,\text{basis}(\mathbf{Y})\right\|_2$

$\boldsymbol{I_T}$: submatrix of identity matrix *I* containing columns with indices in set *T*

- Note: (a) $\kappa_s \leq 1$ (b) Lower the value of κ_s, higher the denseness of the range space. (c) For r-rank Y, $\kappa_1(\boldsymbol{Y}) \geq \sqrt{(\frac{r}{n})}$. (d) $\kappa_1(\boldsymbol{Y}) = \sqrt{\frac{r}{n}}$, if Y is spanned by basis vectors whose entries all have magnitude $\sqrt{\frac{1}{n}}$.

Our research question: How to guarantee $\kappa_s(Y) < \kappa^*$ through signal selection?

[3] H. Guo, C. Qiu, and N. Vaswani, "An Online Algorithm for Separating Sparse and Low-Dimensional Signal Sequences From Their Sum," IEEE Trans. Signal Process., vol. 62, no. 16, pp. 4284–4297, Aug. 2014.
[4] T. T. Cai, L. Wang, and G. Xu, "New bounds for restricted isometry constants," IEEE Trans. Inf. Theory, vol. 56, no. 9, pp. 4388–4394, Sep. 2010.

Corruption-Resilient Signal Selection: Propositions and Lemmas

- Linearized model of power system:

$$\dot{\tilde{\mathbf{x}}}(t) = \mathbf{P}^{-1}\mathbf{A}\mathbf{P}\tilde{\mathbf{x}}(t) + \mathbf{P}^{-1}\mathbf{B}\mathbf{u}(t) = \mathbf{\Lambda}\tilde{\mathbf{x}}(t) + \tilde{\mathbf{B}}\mathbf{u}(t) \quad \mathbf{\Lambda} \in \mathbb{C}^{m\times m} \text{ and } \mathbf{\Psi} \in \mathbb{C}^{n\times m}$$
$$\mathbf{y}(t) = \mathbf{C}\mathbf{P}\tilde{\mathbf{x}}(t) = \mathbf{\Psi}\tilde{\mathbf{x}}(t) \qquad \mathbf{x}(t) \in \Re^{m\times 1},\ \mathbf{y}(t) \in \Re^{n\times 1}, \text{ and } \mathbf{u}(t) \in \Re^{p\times 1}$$

$\mathbf{\Lambda}$: diagonal matrix with eigenvalues of A, $\mathbf{\Psi}$: modal observability matrix

- Lemma I: $\kappa_s(\mathbf{Y}) \le \kappa_s(\mathbf{\Psi}) = \max_{|T|\le s} \left\| (\mathbf{I}_T)^H \mathbf{\Psi}\mathbf{\Psi}^\dagger \right\|_2$

- *Corollary:* For k poorly-damped modes (others sufficiently damped/unobservable)

$$\kappa_s(\mathbf{Y}) \le \kappa_s(\hat{\mathbf{\Psi}}) \text{ where, } \hat{\mathbf{\Psi}} = \begin{bmatrix} \hat{\mathbf{\Psi}}_1 & \hat{\mathbf{\Psi}}_2 & \cdots & \hat{\mathbf{\Psi}}_k \end{bmatrix} \quad \hat{\mathbf{\Psi}}_j = \begin{bmatrix} \psi_j & \overline{\psi}_j \end{bmatrix}$$

- *Remark:* With k poorly-damped modes (others sufficiently damped/unobservable) numerical-$\mathbf{rank}(\mathbf{Y}) \le rank(\hat{\mathbf{\Psi}}) \le 2k$

Connection established between system theoretic notions of modal observability and indices guaranteeing robust recovery – denseness & restricted isometry

Signal selection with same phase relationship

- Lemma II: For a unimodal case, if the entries in ψ_1 have same phase angles, then rank$\left(\widehat{\Psi}\right)$ is 1.
- *Corollary:* $\kappa_1\left(\widehat{\Psi}\right) = \kappa_1(\psi_1)$
- Lemma III: For a unimodal case, the minimum value of $\kappa_1\left(\widehat{\Psi}\right)$ is attained when signals are selected from a coherent group with minimum variance in the magnitudes of relative modal observabilities.
- Effect of large magnitude outlier in observability matrix: (n-1) signals with mean μ and standard deviation σ of observability magnitudes $|\psi_{1i}|$, and 1 outlier $|\psi_{1i}|_{max} = \mu + \rho\sigma$

$$\kappa_1\left(\widehat{\Psi}\right) = \kappa_1(\psi_1) = \frac{1}{\sqrt{1 + \frac{(n-1)(\mu^2 + \sigma^2)}{(\mu + \rho\sigma)^2}}}$$

$\kappa_1\left(\widehat{\Psi}\right)$ increasing function of ρ and decreasing function of n

Example 1

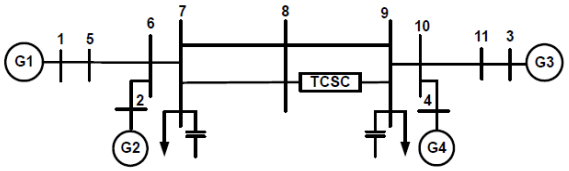

1 poorly-damped inter-area mode with frequency 0.628 Hz and damping ratio 0.012

TABLE I: SIGNALS AND RELATIVE MODAL OBSERVABILITIES

Signals	P_{4-10}	P_{3-11}	P_{11-10}	P_{10-9}
$\lvert\psi_{1i}\rvert$	0.5922	0.6935	0.6935	1.2621
$\angle\psi_{1i}$	$\angle 90°$	$\angle 91°$	$\angle 91°$	$\angle 90°$

Observations:

- $\kappa_1(\hat{\Psi}) = 0.6053$ from our expression, $\kappa_1(Y) = 0.6051$ using Y from nonlinear time-domain simulations → still above κ_1^*
- Add 1 more signal $P_{10\text{-}9}$ with a high $|\boldsymbol{\psi_{1i}}|$ relative to the rest (and thus, ideal for modal estimation) → $\kappa_1(\hat{\Psi}) = 0.7405$, $\kappa_1(Y) = 0.7404$ → worsens

Conclusions:

- Not enough to increase the number of signals – need to minimize variance in $|\boldsymbol{\psi_{1i}}|$
- Might need to sacrifice the 'Best' signal: signal with highest observability

Sacrificing signal with highest observability defies conventional wisdom!!

Example 2

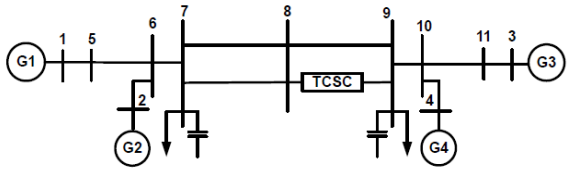

1 poorly-damped inter-area mode with frequency 0.628 Hz and damping ratio 0.012

TABLE II: SIGNALS AND RELATIVE MODAL OBSERVABILITIES

Signals	P_{6-7}	P_{7-8}	P_{8-9}	P_{9-10}	$\theta_7 - \theta_9$
$\lvert\psi_{1i}\rvert$	0.4554	0.4997	0.5064	1.2621	5.0733
$\angle\psi_{1i}$	$\angle -74°$	$\angle -83°$	$\angle -83°$	$\angle -90°$	$\angle -84°$

TABLE III: SIGNALS AND RELATIVE MODAL OBSERVABILITIES

Signals	P_{6-7}	P_{7-8}	P_{8-9}	P_{10-4}	$\theta_4 - \theta_{11}$
$\lvert\psi_{1i}\rvert$	0.4554	0.4997	0.5064	0.5922	0.4500
$\angle\psi_{1i}$	$\angle -74°$	$\angle -83°$	$\angle -83°$	$\angle -90°$	$\angle -84°$

Observations:

- $\angle\boldsymbol{\psi_{1i}}$ are close → rank(Y) ≈ 1, largest singular value: 24.04, second largest: 0.65
- $\theta_7 - \theta_9$: an **outlier** w.r.t. $|\boldsymbol{\psi_{1i}}|$ → $\kappa_1(\hat{\Psi}) = 0.9580$
- Replace $\theta_7 - \theta_9$ by $\theta_4 - \theta_{11}$ and $P_{9\text{-}10}$ by $P_{10\text{-}4}$ → $\sigma = 0.025, \mu = 0.447, \rho = 4.51$, $\kappa_1(\hat{\Psi}) = 0.5262$ → LESS THAN $\boldsymbol{\kappa}^*$ GUARANTEES 1-sparse recovery!!
- If signals are selected such that the variation in observability magnitudes is small $\left(\frac{\mu}{\sigma} \gg 1, \rho \approx 1\right)$; $\kappa_1(\hat{\Psi}) = \kappa_1(\psi_1) \approx \frac{1}{\sqrt{n}}\left(1 + \frac{\rho\sigma}{\mu}\right)$
- $\frac{\mu}{\sigma} = 18.83 \gg \rho$, $\kappa_1(\hat{\Psi}) \approx 0.554$

For sufficiently dense vectors, κ_1 increases linearly with ρ and σ

Example 2 (Contd…): Parameter Manipulation Attack

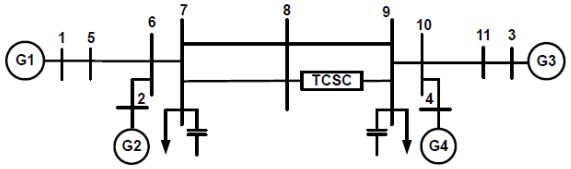

1 poorly-damped inter-area mode with frequency 0.628 Hz and damping ratio 0.012

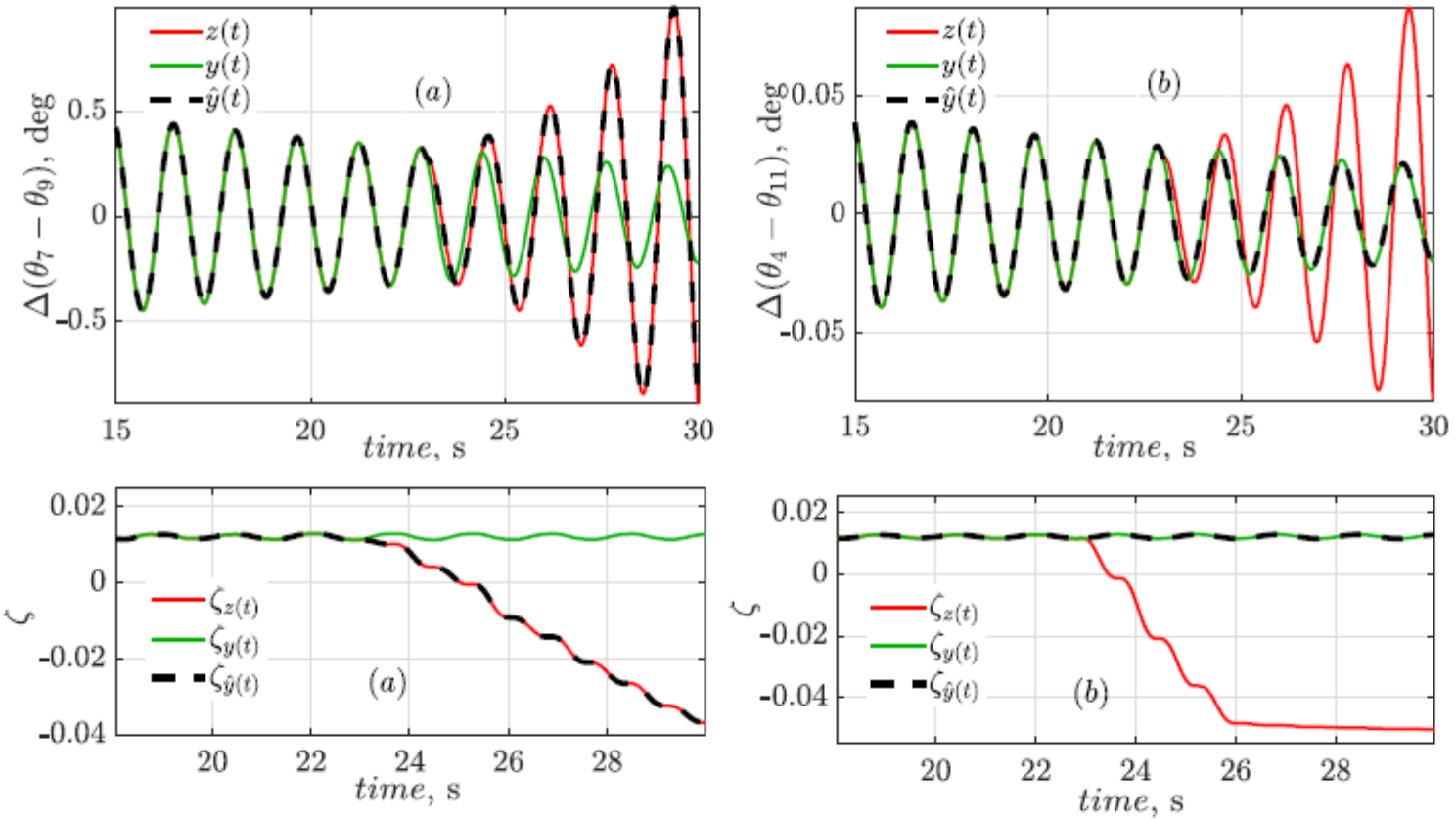

Damping and frequency plots using multichannel Prony [5]

[5] D. J. Trudnowski, J. M. Johnson, and J. F. Hauer, "Making Prony Analysis More Accurate using Multiple Signals," IEEE Trans. Power Syst., vol. 14, no. 1, pp. 226–231, Feb. 1999.

Example 2 (Contd…): Missing Data Attack

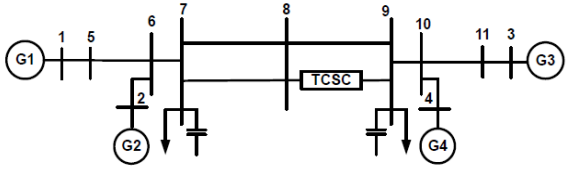

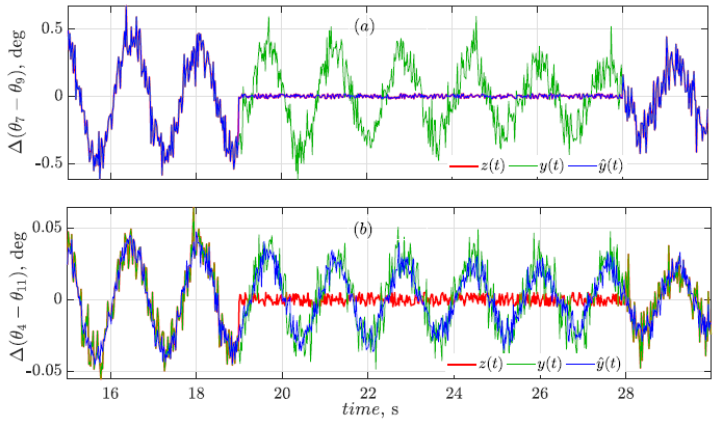

1 poorly-damped inter-area mode with frequency 0.628 Hz and damping ratio 0.012

TABLE V: MODAL ESTIMATION USING MULTI-CHANNEL PRONY ON NOISY SIGNALS IN TABLE II WITH MISSING DATA ATTACK ON $\Delta(\theta_7-\theta_9)$ AND AFTER RECOVERY FOR DIFFERENT NOISE LEVELS

SNR (dB)	With Corruption		After Recovery	
	mean ζ ± std. dev.	mean f (Hz) ± std. dev.	mean ζ ± std. dev.	mean f (Hz) ± std. dev.
60	0.0630 ± 0.0012	0.627 ± 0.0047	0.0610 ± 0.0017	0.625 ± 0.0086
50	0.0677 ± 0.0011	0.624 ± 0.0080	0.0626 ± 0.0036	0.625 ± 0.0053
40	0.0640 ± 0.0007	0.625 ± 0.0051	0.0621 ± 0.0019	0.625 ± 0.0073

TABLE VI: MODAL ESTIMATION USING MULTI-CHANNEL PRONY ON NOISY SIGNALS IN TABLE III WITH MISSING DATA ATTACK ON $\Delta(\theta_4-\theta_{11})$ AND AFTER RECOVERY FOR DIFFERENT NOISE LEVELS

SNR (dB)	With Corruption		After Recovery	
	mean ζ ± std. dev.	mean f (Hz) ± std. dev.	mean ζ ± std. dev.	mean f (Hz) ± std. dev.
60	0.0277 ± 0.0017	0.633 ± 0.0068	0.0127 ± 0.0011	0.628 ± 0.0032
50	0.0274 ± 0.0020	0.637 ± 0.0055	0.0128 ± 0.0014	0.628 ± 0.0022
40	0.0260 ± 0.0027	0.632 ± 0.0088	0.0121 ± 0.0016	0.629 ± 0.0062

Incorrect recovery leads to appearance of well-damped system

Generic Signal Selection for Unimodal Case

- Generic Signal Selection for Unimodal Case: $\text{Rank}(\widehat{\Psi}) = 2$, $\min(\kappa_1) = \sqrt{\frac{2}{n}}$
- Lemma IV: If the entries in ψ_1 are such that $\langle \psi_1, \bar{\psi}_1 \rangle = 0$, then $\kappa_1(\widehat{\Psi}) = \sqrt{2}\kappa_1(\psi_1)$
- Lemma V: If signals are selected such that the variation in observability magnitudes is small $\left(\frac{\mu}{\sigma} \gg \rho\right)$ and the absolute value of the inner product $\left|\langle \psi_1, \bar{\psi}_1 \rangle\right| \leq \epsilon$ for some ϵ, then

$$\kappa_1(\widehat{\Psi}) \leq \sqrt{\frac{2}{n}\left(1 + \frac{\rho\sigma}{\mu}\right)\left(1 + \frac{\epsilon}{2\|\psi_1\|_2^2}\right)}$$

$\langle \psi_1, \bar{\psi}_1 \rangle = 0$ is hard to achieve, so Lemma V is formulated

Example 3

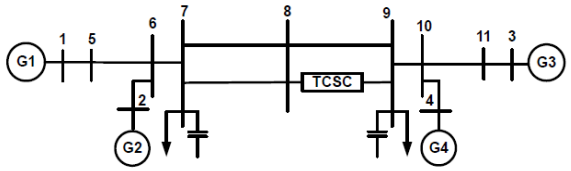

1 poorly-damped inter-area mode with frequency 0.628 Hz and damping ratio 0.012

TABLE VII: SIGNALS AND RELATIVE MODAL OBSERVABILITIES

Signals	$\theta_3 - \theta_{11}$	P_{3-11}	P_{11-10}	$f_1 - f_3$	$f_2 - f_3$
$\lvert\psi_{1i}\rvert$	0.6340	0.6935	0.6935	0.8231	0.7501
$\angle\psi_{1i}$	$\angle 84.1°$	$\angle 91°$	$\angle 91°$	$\angle 3.5°$	$\angle 3.8°$

1. Signals in two groups almost in quadrature
2. Relative magnitudes are close by

Observations:

- $\angle\boldsymbol{\psi_{1i}}$ are significantly different → rank(Y) ≈ 2
- $\kappa_1(\hat{\Psi}) = 0.7385$, $\kappa_1(Y) = 0.7377$
- In this case, $\left|\langle\psi_1, \bar{\psi}_1\rangle\right| = \epsilon = 0.138$ and $\epsilon^2 / \left|\left|\psi_1\right|\right|_2^4 = 0.0028 << 1$, $\sigma = 0.041, \mu = 0.693, \rho = 3.19$
- $\kappa_1(\hat{\Psi}) <$ 0.7711 FROM LEMMA V

Validates proposition on upper bound on denseness due to a small non-zero perturbation in inner product

Signal Selection for Multiple Modes

- Minimal variation in observability phase angle and magnitudes for <u>each mode</u>
- Basis vector corresponding to the largest singular value captures most of the variance → numerical-rank (Y) ≈1

TABLE IX: MODE-WISE DENSENESS[2] OF $|V_1|, |V_8|, |V_6|$, and $|V_7|$

Modes	0.51 Hz	0.39 Hz	0.62 Hz	0.79 Hz
$\kappa_1(\hat{\Psi}_i)$	0.5959	0.5470	0.5765	0.9968

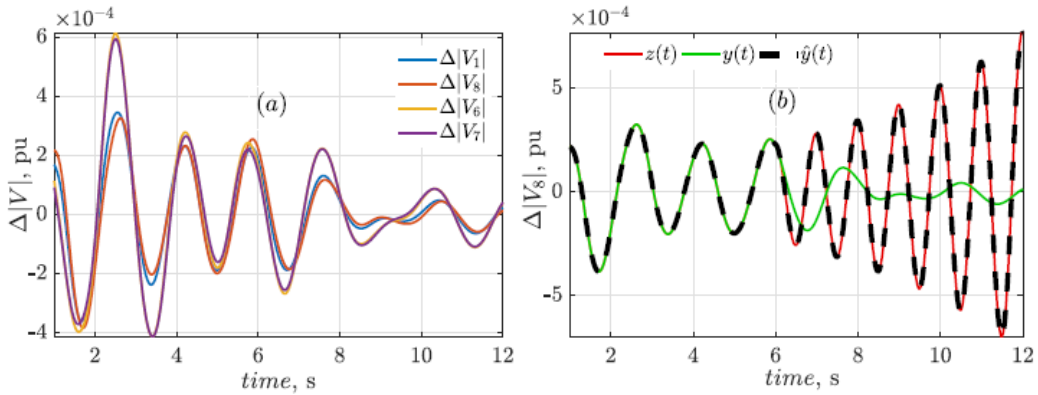

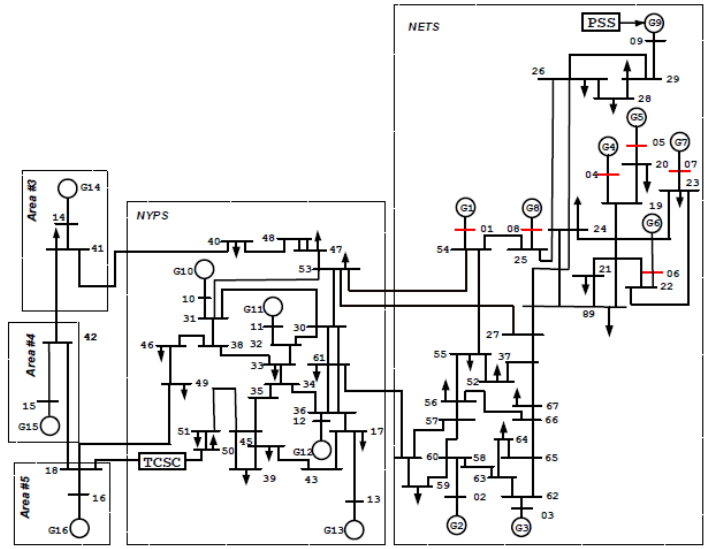

Fig. 5: IEEE 5−area 16-machine New England - New York test system.

Incorrect recovery with parameter manipulation attack

Signal Selection for Multiple Modes

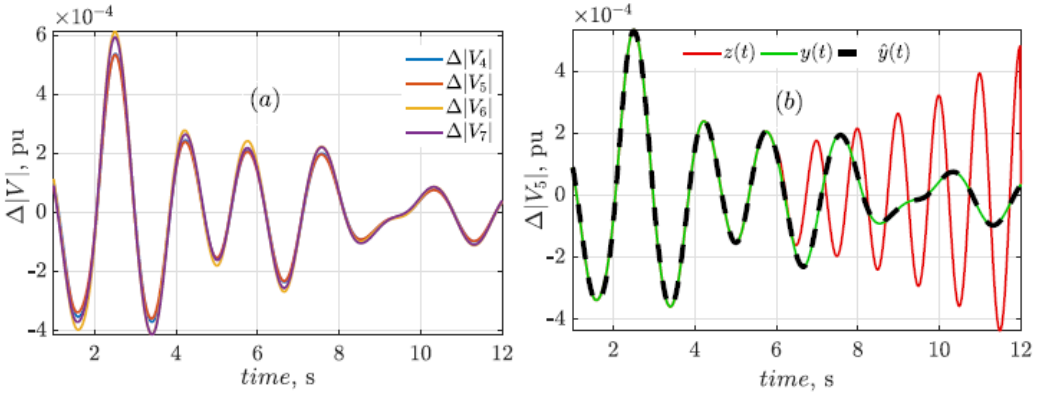

TABLE X: MODE-WISE DENSENESS[2] OF $|V_4|, |V_5|, |V_6|$, and $|V_7|$

Modes	0.51 Hz	0.39 Hz	0.62 Hz	0.79 Hz
$\kappa_1(\Psi_i)$	0.5328	0.5229	0.5377	0.5519
$\frac{1}{\sqrt{n}}\left(1+\frac{\rho_i\sigma_i}{\mu_i}\right)$	0.5468	0.5322	0.5541	0.5761

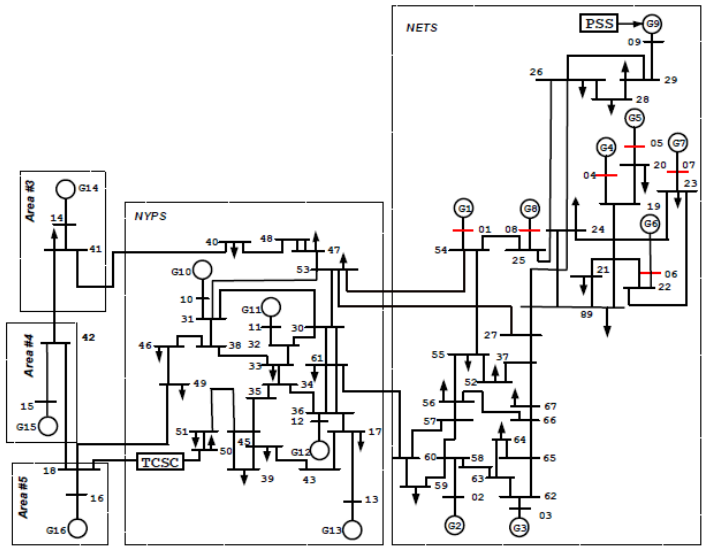

Fig. 5: IEEE 5−area 16-machine New England - New York test system.

- Overall denseness $\kappa_1(\hat{\Psi}) = 0.5359 < \boldsymbol{\kappa}^*$
- Note: Ideally, $\kappa_1(\hat{\Psi}) \geq \kappa_1(\hat{\Psi}_i), \forall i \leq k$ Here, truncation is applied since largest singular vector captures 97% variance

|V1|, |V8| replaced by |V4|, |V5|: Correct recovery with parameter manipulation attack

Signal Selection from NYPA Data

- Detrended voltage magnitudes $|V_1|$-$|V_{40}|$: $\kappa_1(Y) = 0.549$ → guarantees 1-sparse recovery in 40 signals – Awfully inadequate
- No linear model: Purely data-driven approach for signal selection
- Spectral decomposition gives 2 modes: 0.06 Hz and 0.25 Hz
- Output-to-output TF approach [6] used to calculate relative modeshapes --- equivalent to relative observabilities
- Group signals to attain minimum variance in magnitudes and angles of observabilities for each mode: clustering algorithms can be used

TABLE XII: SIGNAL SETS I AND II

Signal Set I	$\|V_6\|$, $\|V_{15}\|$, $\|V_{19}\|$, $\|V_{20}\|$, $\|V_{21}\|$, $\|V_{26}\|$, $\|V_{27}\|$, $\|V_{28}\|$
Signal Set II	$\|V_4\|$, $\|V_7\|$, $\|V_{11}\|$, $\|V_{13}\|$, $\|V_{16}\|$, $\|V_{17}\|$, $\|V_{22}\|$, $\|V_{24}\|$

Goal: Group signals such that at least 1-sparse recovery is guaranteed in each

[6] L. Dosiek, N. Zhou, J. W. Pierre, Z. Huang, and D. J. Trudnowski, "Mode Shape Estimation Algorithms under Ambient Conditions: A Comparative Review," IEEE Trans. on Power Syst., vol. 28, no. 2, pp. 779–787, May 2013.

Signal Selection from NYPA Data

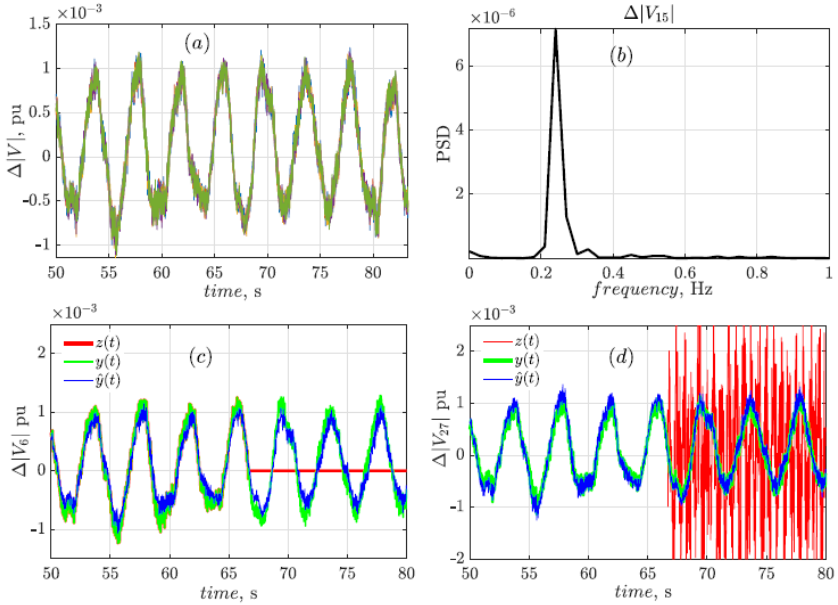

Fig. 8: Plots for (a) all signals in set I prior to corruption with (b) PSD, and (c)-(d) correct 2−sparse recovery after corruption of $|V_6|$ and $|V_{27}|$.

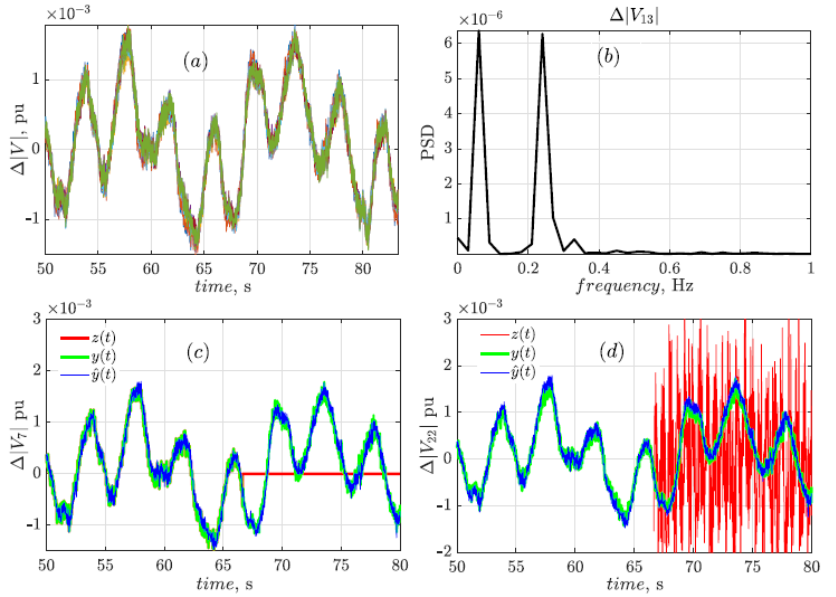

Fig. 9: Plots for (a) all signals in set II prior to corruption with (b) PSD, and (c)-(d) correct 2−sparse recovery after corruption of $|V_7|$ and $|V_{22}|$.

Group	$\kappa_1(\mathbf{Y})$	$\kappa_1(\hat{\mathbf{\Psi}})$	$\kappa_2(\mathbf{Y})$	$\kappa_2(\hat{\mathbf{\Psi}})$
Signal Set I	0.3806	0.4109	0.5382	0.5530
Signal Set II	0.3752	0.3804	0.5275	0.5363

Freq.	$\kappa_1(\hat{\mathbf{\Psi}}_\mathbf{i})$	$\frac{1}{\sqrt{n}}(1+\frac{\rho_i\sigma_i}{\mu_i})$	$\kappa_2(\hat{\mathbf{\Psi}}_\mathbf{i})$	$\sqrt{\frac{2}{n}}(1+\frac{\rho_i\sigma_i}{\mu_i})$
0.25 Hz	0.3794	0.3842	0.5259	0.5433
0.06 Hz	0.3884	0.3953	0.5438	0.5590

Denseness coefficients satisfy analytical bounds: Sets I and II meet $\kappa_s < 0.554$ – guaranteed reconstruction for corruption in 2 out of 8 signals!

Mode Meter Result from NYPA Data

TABLE XV:
ESTIMATION OF 0.25 Hz OSCILLATION FROM $\Delta|V_6|$ AND $\Delta|V_{27}|$ – WITH CORRUPTION AND AFTER RECOVERY USING SIGNAL SET I

Parameters	Prony on $\Delta\|V_6\|$			Prony on $\Delta\|V_{27}\|$		
	$y(t)$	$z(t)$	$\hat{y}(t)$	$y(t)$	$z(t)$	$\hat{y}(t)$
Damp. Ratio	0.026	0.069	0.026	0.023	0.078	0.025
Freq. (Hz)	0.250	0.216	0.251	0.251	0.211	0.251

TABLE XVI:
ESTIMATION OF 0.25 Hz OSCILLATION FROM $\Delta|V_7|$ AND $\Delta|V_{22}|$ – WITH CORRUPTION AND AFTER RECOVERY USING SIGNAL SET II

Parameters	Prony on $\Delta\|V_7\|$			Prony on $\Delta\|V_{22}\|$		
	$y(t)$	$z(t)$	$\hat{y}(t)$	$y(t)$	$z(t)$	$\hat{y}(t)$
Damp. ratio	0.025	0.113	0.027	0.024	0.104	0.023
Freq. (Hz)	0.251	0.214	0.251	0.251	0.212	0.251

Corruption resilience of mode meter is evident

Signal Selection from NYPA Data (Contd.)

Signal Set III	$\lvert V_{15}\rvert,\ \lvert V_{20}\rvert,\ \lvert V_{21}\rvert,\ \lvert V_{27}\rvert,\ \lvert V_{4}\rvert,\ \lvert V_{11}\rvert,\ \lvert V_{7}\rvert,\ \lvert V_{22}\rvert$

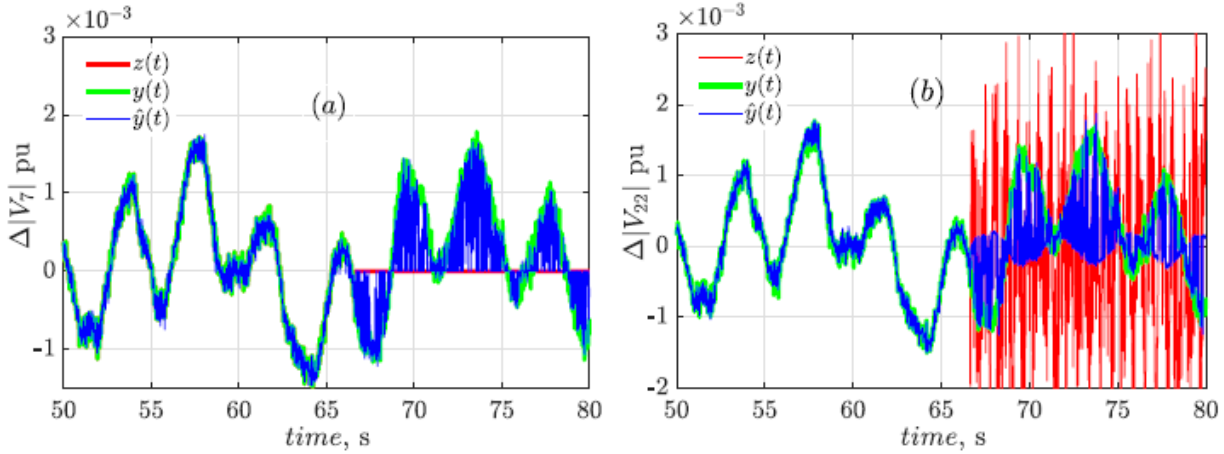

$$\kappa_1(Y) = 0.709, \kappa_2(Y) = 0.995$$

Set III does not meet $\kappa_s < 0.554$

Conclusion

- Insights into PMU signal grouping was developed to enhance denseness of a set
- Grouping can be model based or data driven
- Link between denseness and modal observability was established
- Denseness increases when signals were grouped with observabilities in same phase and variance in magnitude is minimized
- Conventionally preferred (high observability) signals might have to be sacrificed for guaranteed recovery from corruption

References

- J6. K. Chatterjee, N. R. Chaudhuri, and G. Stefopoulos, “Signal Selection for Oscillation Monitoring with Guarantees on Data Recovery under Corruption,” IEEE Transactions on Power Systems, vol. 35, no. 6, pp. 4723 – 4733, Nov. 2020.
- J5. K. Chatterjee, K. Mahapatra, and N. R. Chaudhuri, “Robust Recovery of PMU Signals with Outlier Characterization and Stochastic Subspace Selection,” IEEE Transactions on Smart Grid, IEEE Transactions on Smart Grid, vol. 11, no. 4, pp. 3346 – 3358.
- J4. K. Mahapatra, M. Ashour, N. R. Chaudhuri, and C. Lagoa, “Malicious Corruption Resilience in PMU Data and Wide Area Damping Control,” IEEE Transactions on Smart Grid, vol. 11, no. 2, pp. 958 – 967.
- J3. K. Mahapatra, and N. R. Chaudhuri, “Online Robust PCA for Malicious Attack-Resilience in Wide-Area Mode Metering Application,” IEEE Transactions on Power Systems, vol. 34 , no. 4 , pp. 2598 – 2610.
- J2. K. Mahapatra and N. R. Chaudhuri, “Malicious Corruption-Resilient Wide-Area Oscillation Monitoring using Principal Component Pursuit,” IEEE Transactions on Smart Grid, vol. 10, no. 2, pp. 1813 – 1825.
- J1. K. Mahapatra, N. R. Chaudhuri, R. Kavasseri, and S. Brahma, “Online Analytical Characterization of Outliers in Synchrophasor Measurements: A Singular Value Perturbation Viewpoint,” IEEE Transactions on Power Systems, vol. 33, no. 4, pp. 3863-3874.
- C4. K. Chatterjee and N.R.Chaudhuri, “Distributed Anomaly Detection and PMU Data Recovery in a Fog-computing-WAMS Paradigm (Invited Paper),” to be presented in IEEE SmartGridComm 2020, pp. 1-6.
- C3. K. Chatterjee, N.R.Chaudhuri, and G. Stefopoulos, “Grouping PMU Signals for Guaranteed Recovery under Corruption: Insights and Recommendations,” to be presented in IEEE PES General Meeting, Montreal, QC, Canada, pp. 1-5.
- C2. K. Chatterjee, and N.R.Chaudhuri, “Corruption-Resilient Detection of Event-Induced Outliers in PMU Data: A Kernel PCA Approach,” in proceedings of 2019 IEEE PES General Meeting, Atlanta, GA, pp. 1-5. (selected among the Best Conference Papers)
- C1. K. Mahapatra, and N.R.Chaudhuri, “Malicious Corruption-Resilient Wide-Area Oscillation Monitoring using Online Robust PCA,” in proceedings of 2018 IEEE PES General Meeting, Portland, OR.

SUstainable Power & Energy Research Group (SUPER Group)

Funding from NSF grant award CNS1739206 and field PMU data from NYPA gratefully acknowledged

Thank You!

PennState College of Engineering

EECS